

Recoil range distributions of residues from $\alpha + {}^{59}\text{Co}$ reactions

E. Gadioli and E. Gadioli Erba

Dipartimento di Fisica dell'Universita' di Milano

and Istituto Nazionale di Fisica Nucleare, Sezione di Milano, 20133 Milano, Italia

D. J. Parker and J. Asher

Nuclear Physics Division, Atomic Energy Research Establishment, Harwell, Oxfordshire, OX11 0RA, United Kingdom

(Received 22 April 1985)

The recoil range distributions of ${}^{61}\text{Cu}$, ${}^{60}\text{Cu}$, ${}^{58}\text{Co}$, ${}^{57}\text{Co}$, ${}^{56}\text{Co}$, ${}^{54}\text{Mn}$, and ${}^{52}\text{Mn}$ residual nuclei produced in α particle bombardment of ${}^{59}\text{Co}$ at 38, 50, 65, and 85 MeV have been measured and analyzed. Analysis of these measurements, as well as other recently published measurements of longitudinal linear momentum transfer to residue isobars at energies extending up to ≈ 200 MeV, in the same reaction, shows that calculations based on the exciton model and a realistic description of the α -nucleus interaction allow a quantitatively correct description of α -induced reactions. Contrary to recent suggestions, data of this kind do not seem to indicate a change in the general character of the α -nucleus interaction for incident energies below ≈ 50 MeV/nucleon.

I. INTRODUCTION

The value of measurements of the recoil range distributions of radioactive spallation residues, in nuclear reaction studies, has been appreciated since the late 1950's.

The velocity distribution of the residue after a reaction provides an indication of the mechanism by which it was formed. In fact, the recoil velocity reflects the degree of momentum transfer from the projectile. The transfer will be maximum in complete fusion processes and will be correspondingly reduced in *direct*, *preequilibrium*, and *break-up* processes when a large fraction of the incident momentum is carried off by fast particles emitted at an early stage of the reaction.

Most of the studies reported in the literature comprise measurements of the mean recoil ranges of given residuals, projected along the beam axis, in thick target-thick catcher experiments. These data, together with measurements of the velocity distribution of residues by time of flight techniques and of the correlation of fission fragments in the case of heavy nuclei, indicate that the percentage of mean longitudinal linear momentum transfer, in light ion ($A < 20$)-nucleus interactions, decreases linearly over the energy range from 0 to ≈ 70 – 80 MeV/nucleon.¹

Although this result is of great relevance, it must be stressed that this experimental information alone is not sufficient to provide a clear indication of the reaction mechanism, and theoretical approaches based on various physical assumptions might lead to similar estimates of the mean linear momentum transferred, which may only be resolved by means of more detailed measurements.

Measurements of differential range distributions of reaction residues, which provide much more detailed information on the reaction mechanism, are quite scarce and their accuracy has in the past been limited by the nonuniformity of the catcher foils used; these were generally made from aluminum leaf which is known to be extreme-

ly nonuniform.

This paper reports the results of measurements of differential projected range distributions, using highly uniform thin evaporated aluminum catchers, for α particle reactions on ${}^{59}\text{Co}$ at energies up to 85 MeV. Application of this technique to α -induced reactions is intrinsically more difficult than for the heavy ion reactions previously studied,² because the momentum transfer is lower and the recoil ranges are correspondingly shorter.

The measured recoil range distributions provide a more detailed test of a model that has previously been used to reproduce measured excitation functions and emitted particle spectra for α -particle-induced reactions.³

These calculations also successfully reproduce recently published data¹ on mean recoil momenta of residue isobars from the same reactions at higher energies, implying that, in contrast to recent suggestions,¹ no new process is required to explain these.

II. EXPERIMENTAL TECHNIQUE

Projected range distributions for seven nuclides (${}^{61}\text{Cu}$, ${}^{60}\text{Cu}$, ${}^{58}\text{Co}$, ${}^{57}\text{Co}$, ${}^{56}\text{Co}$, ${}^{54}\text{Mn}$, and ${}^{52}\text{Mn}$) were measured by irradiating a thin ${}^{59}\text{Co}$ target mounted in front of a stack of typically 20 thin aluminum catcher foils. Subsequently, γ -ray spectrometry was used to determine the distribution through the catcher stack of products from the target.

The target consisted of a layer of about $100 \mu\text{g cm}^{-2}$ of cobalt deposited by evaporation in vacuum onto a self-supporting aluminum foil about $100 \mu\text{g cm}^{-2}$ thick; the catchers used were self-supporting aluminum foils produced by evaporation of aluminum onto glass slides in vacuum. The thickness of aluminum deposited was first monitored using a crystal oscillator deposition monitor mounted alongside the slides, then a more accurate determination was achieved by measuring the energy lost in traversing each aluminum foil by 5.806 MeV α particles from a ${}^{244}\text{Cm}$ source.

The catcher foils were mounted on annular tantalum holders with an inside diameter of 15 mm, and the target and typically 20 catchers were stacked in a close geometry inside a Faraday cup on the end of the beam line, with the cobalt target layer downstream of the aluminum support foil. Further details of the experimental technique may be found elsewhere.⁴ The stack of foils was irradiated with an α beam extracted from the Harwell Variable Energy Cyclotron, collimated to a spot diameter of 5 mm with a divergence of less than 0.5° . In different irradiations, α particle energies of 38, 50, 65, and 85 MeV were used. In order to avoid overheating the stack, the beam flux was limited to 50 particle nA. Each activation lasted typically 4–6 h, and involved a total fluence of approximately 1000 particle μC .

The counting of the activity induced in the catcher foils and the target commenced within half an hour of the end of irradiation, each foil being counted for, typically, 200 s. After the first sequence of counts, the foils were recounted in turn for typically 400 s, to study products with half-lives of a few hours. They were again recounted within the next few days. The final count commenced several weeks after irradiation and involved counting each catcher for typically 24 h. Since the yield of the activities of interest was necessarily small, due to the use of a thin target and the fact that the products were spread over several catchers, the foils were counted resting on the casing of a 25% efficient vertical coaxial Ge(Li) detector, to achieve the maximum counting efficiency.

In this close counting geometry, there is a significant probability that the Ge(Li) will detect more than one of the radiations emitted in rapid succession by a particular radioactive nucleus (electron/positrons and one or more γ rays) and will not be able to resolve them as distinct events, so that they become summed and events are lost from the measured γ -ray photopeaks. The effective photopeak efficiency is thus extremely sensitive to the precise details of the decay scheme of the radioisotopes being counted, and it is certainly not possible to use a universal curve of efficiency vs γ -ray energy for all radioactive products. For this reason, no attempt was made to obtain absolute cross section data directly in this study.

The distribution of the products of interest through the catcher stack was determined by selecting, for each product, a characteristic γ -ray energy (see Table I) that could be unambiguously attributed to this product and counting the relative intensity of this photopeak in each catcher.

TABLE I. Half-lives of radioactive nuclei studied in this work and energies of γ rays utilized for their identification.

Isotope	Half-life	E_γ (keV)
^{61}Cu	3.41 h	283
^{60}Cu	23.2 min	1332
^{58}Co	70.8 d	810
^{57}Co	270.9 d	122
^{56}Co	78.8 d	846
^{54}Mn	312.5 d	835
^{52}Mn	5.59 d	744

The relative uncertainty in the yields measured within each range distribution is estimated to be $\approx 5\text{--}10\%$ and is mainly due to the uncertainty in catcher thickness.

The absolute cross sections were obtained by normalization of the integrals of the measured distributions to the values obtained in previous thick target measurements of the corresponding excitation functions.^{3,4}

This normalization procedure would give incorrect results if some of the yield of a particular product was not collected in the stack. The most likely reason for this would be if the recoil ranges were so low that some products did not emerge from the target layer, or if indeed the recoil velocities were opposed to beam velocity. Even in this case it is almost certain that the recoil velocity would be so low that any product would stop in the support layer before the target. Thus, in order to achieve correct normalization, it was, in general, necessary to count the activity induced in the combined support/target foil as well as in the catchers, and to include any yield found in this

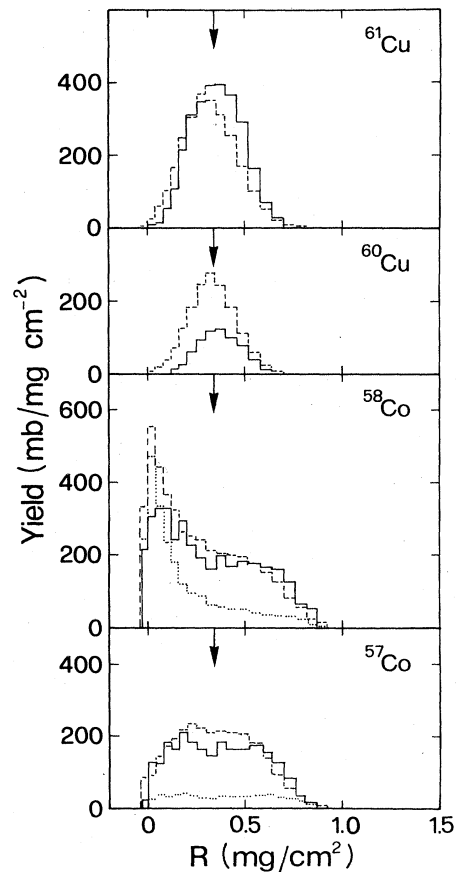


FIG. 1. Comparison between measured (continuous line histograms) and calculated (dashed line histograms) projected range distributions of ^{61}Cu , ^{60}Cu , ^{58}Co , and ^{57}Co residues in α particle bombardment of ^{59}Co at 38 MeV. Here and in the following three figures, the contribution of processes involving the pre-equilibrium emission of an α particle is given by the dotted histograms and the arrows indicate the expected value of the mean recoil range in a purely compound nucleus process.

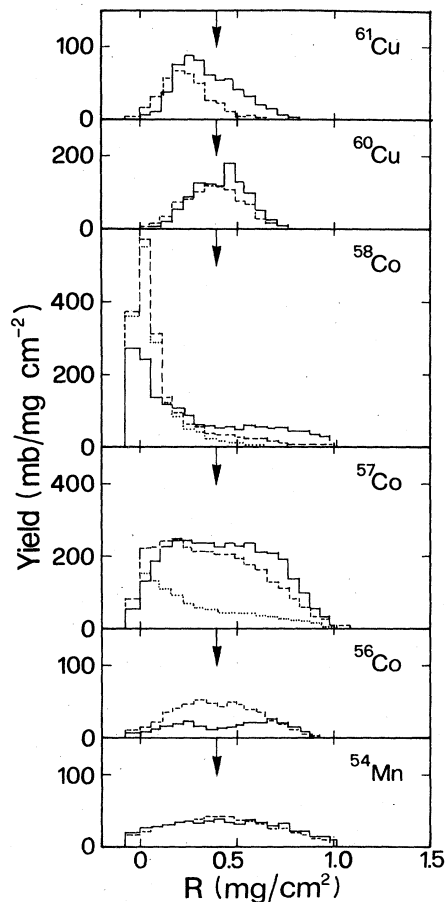


FIG. 2. Comparison between measured (continuous line histograms) and calculated (dashed line histograms) projected range distributions of ^{61}Cu , ^{60}Cu , ^{58}Co , ^{57}Co , ^{56}Co , and ^{54}Mn residues in α particle bombardment of ^{59}Co at 50 MeV. In the case of ^{56}Co and ^{54}Mn , emission of a preequilibrium α particle gives a rather small contribution to the range distribution, never exceeding 15–20% of the calculated yield.

foil in the total yield. In Figs. 1–4, the yield in the combined support/target foil is shown in the first bin of each histogram (recoil range ≤ 0).

III. ANALYSIS OF EXPERIMENTAL DATA

The measured recoil range distributions are shown in Figs. 1–4.

Excitation functions for production of 14 radioactive residual nuclides and the emitted proton and α particle spectra have already been measured,^{3–5} for α energies varying from 10 to 170 MeV, and analyzed in the framework of the exciton model.³ These studies indicated the importance of preequilibrium processes in α -nucleus interactions. The present data confirm these conclusions

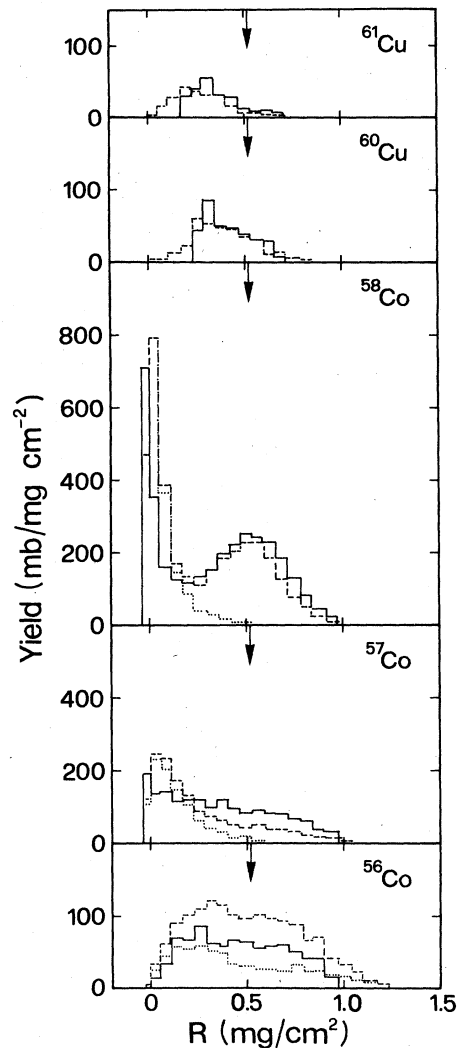


FIG. 3. Comparison between measured (continuous line histograms) and calculated (dashed line histograms) projected range distributions of ^{61}Cu , ^{60}Cu , ^{58}Co , ^{57}Co , and ^{56}Co residues in α particle bombardment of ^{59}Co at 65 MeV.

and perhaps allow a more direct separation between preequilibrium and compound nucleus processes.

If all the residues were produced in compound nucleus processes, all the range distributions would be approximately symmetrical around a mean recoil range that would be approximately the same for all residues (the range corresponding to the recoil velocity of the compound nucleus). The width of the distribution arises from the evaporation from the compound nucleus. Emission of α particles causes a greater perturbation of the recoil velocity, and therefore a greater width in the range distributions, than emission of individual nucleons. This effect is seen, for example, in the case of ^{58}Co ; at the lower energies where evaporation of an α and a neutron is most important, the intrinsic width of the compound nucleus component of the range distribution is greater than at 65 and 85 MeV where evaporation of five separate nucleons occurs.

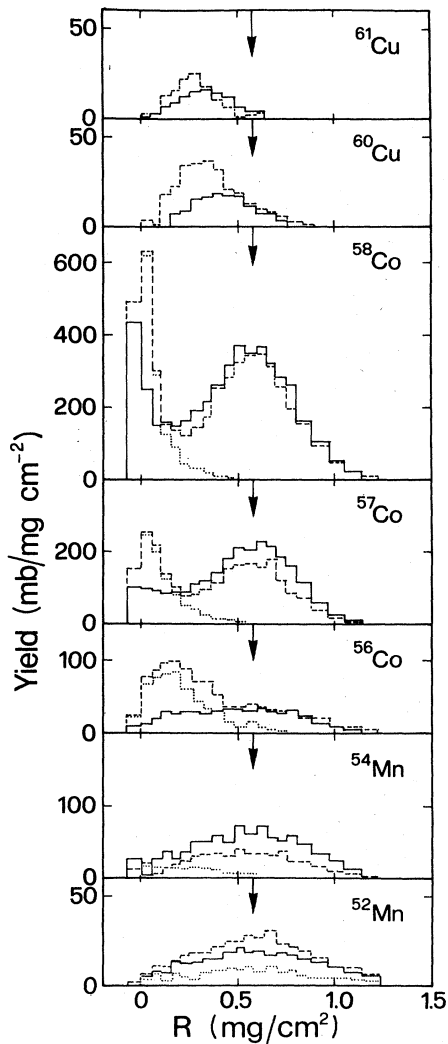


FIG. 4. Comparison between measured (continuous line histograms) and calculated (dashed line histograms) projected range distributions of ^{61}Cu , ^{60}Cu , ^{58}Co , ^{57}Co , ^{56}Co , ^{54}Mn , and ^{52}Mn residues in α particle bombardment of ^{59}Co at 85 MeV.

It is clearly seen that several of the distributions cannot simply be accounted for by evaporation from the compound nucleus. For instance, even at 38 MeV, the ^{58}Co distribution shows a peak at a range considerably smaller than the mean range characterizing the other distributions. At this energy, although the main contribution to the cross section for production of this isotope is evaporation of one α particle and a neutron, the low energy peak reveals the presence of noncompound processes. This peak dominates the ^{58}Co distribution at 50 MeV (where compound nucleus processes do not strongly populate this product). At the higher incident energies, compound nucleus processes again become important with the evaporation of individual nucleons. The low range component may easily be explained in terms of preequilibrium emission of high energy α particles, in the deexcitation process producing the ^{58}Co radioactive residual. The 85 MeV distribution is a clear example of the value of such experi-

mental results in elucidating the nature of reaction processes. From the excitation function for production of ^{58}Co at this energy (see Fig. 5) the contribution, to the measured cross section, of the reaction path involving the emission of a high energy preequilibrium α particle is not obvious, whereas it is clearly apparent from the measured recoil range distribution.

At 65 and 85 MeV the mean recoil range characterizing the ^{61}Cu and ^{60}Cu distributions is considerably smaller than the center of the broad peak in the ^{58}Co distribution which, as already explained, corresponds to compound nucleus processes. This indicates that at least one of the neutrons emitted during the deexcitation process producing the ^{61}Cu and ^{60}Cu nuclei has been emitted during the preequilibrium phase. The lack of symmetry of the ^{57}Co and ^{56}Co distributions at 65 MeV also indicates the importance of preequilibrium decay.

As mentioned above, the excitation functions for the reactions considered here have already been quite successfully reproduced by exciton model calculations, using the code OMEGA. This theoretical approach has been discussed in detail in Refs. 3, 6, and 7 and further improvements were described in Ref. 8. To summarize, this calculation considers several distinct initial interaction modes for the α particle. In order of importance these are the following:

- (a) two-body interaction of the incident α particle with nucleons of the target,
- (b) dissolution of the α into four captured nucleons, in the field of the target nucleus,
- (c) binary fragmentation with capture of one fragment,
- (d) inelastic scattering with excitation of low-lying collective states and giant resonances.

Each of these initial interaction modes initiates an intranuclear deexcitation cascade during which preequilibrium emission of α particles and nucleons may occur. Figure 6 shows the estimated contributions, to the total α -nucleus reaction cross section, of the cumulative cross sections of processes initiated by these four interaction modes. These estimates do not practically differ from the ones previously reported in Ref. 3 and are shown here only for the sake of completeness. They are obtained through a detailed comparison of model predictions with independent experimental data as discussed in Refs. 7 and 8. For instance, the total cross section for α particle fragmentation to four nucleons is deduced from the yield of the highest energy part of experimental inclusive proton spectra; the total cross section for processes initiated by α -nucleon interactions may be estimated from the analysis of the medium energy region of the inclusive spectra of inelastically scattered α particles.

Our estimate of the contribution of different α -nucleon interaction modes is rather different from that of other authors. For a comparison of the present approach with other theoretical models we refer to Refs. 7 and 8.

As previously mentioned, the range distribution data allow a further detailed check of our calculations and also an extension of the model used.

In fact, the previous OMEGA calculations, concerned

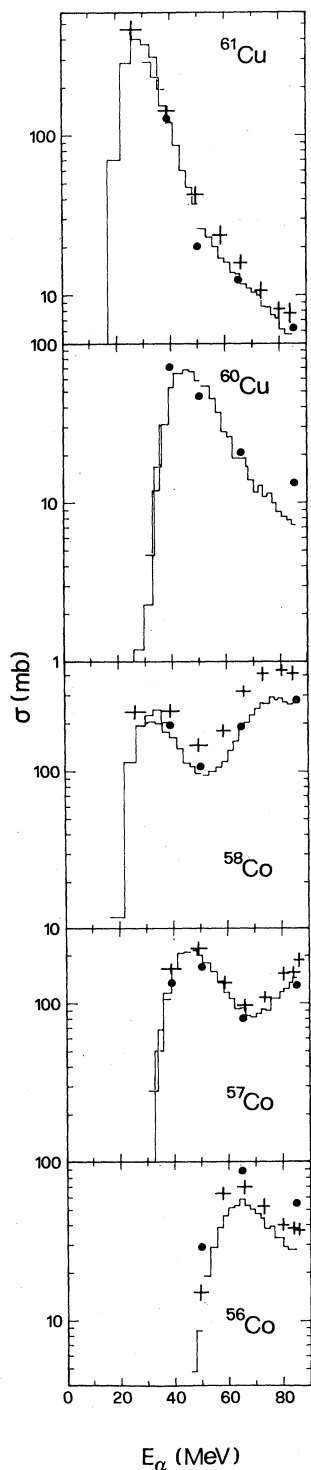


FIG. 5. Comparison between measured and calculated excitation functions for production of ^{61}Cu , ^{60}Cu , ^{58}Co , ^{57}Co , and ^{56}Co . The histograms and the points with horizontal and vertical error bars represent the experimental results reported, respectively, in Refs. 3 and 5. The results of the present calculation are given by the black dots.

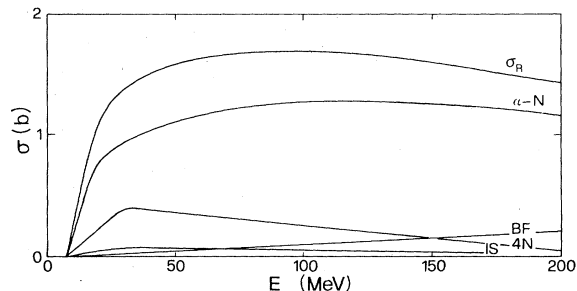


FIG. 6. Estimated contributions to the total α -nucleus reaction cross section, σ_R , of the cumulative cross sections of processes originated from (a) α -nucleon interactions (α -N), (b) dissolution into four nucleons (4N), (c) binary fragmentation (BF), (d) inelastic scattering to low energy collective states and giant resonances (IS).

mainly with the study of excitation functions and angle integrated energy spectra, considered only the energy distribution of the emitted particles. In the present analysis of projected recoil ranges, it is also necessary to take their angular distribution explicitly into account.

The angular distribution of α particles emitted in the preequilibrium phase may be calculated in the framework of the model adopted here; results of calculations of this kind were reported in Refs. 6 and 8. These angular distributions are rather accurately reproduced by an exponential function of the type

$$\sigma(\theta, \phi) \propto \exp \left[\frac{-\theta}{A(E_{\text{inc}}, E_{\text{out}})} \right], \quad (1)$$

where θ is the angle between the linear momentum of the emitted particle and the linear momentum of the emitting nucleus. A similar result is obtained for the angular distribution of the nucleons emitted during the preequilibrium phase, assuming that they result mainly from the interaction of one nucleon from the fragmentation of the alpha with a nucleon of the target.

In order to improve the accuracy, instead of evaluating $A(E_{\text{inc}}, E_{\text{out}})$ with our model, we used values obtained from a fit to experimental angular distributions of preequilibrium nucleons and α 's reported in the literature for $A \approx 60$ nuclei, at various incident energies. The expression, adopted in this work, for $A(E_{\text{inc}}, E_{\text{out}})$, as a function of the incident α energy, E_{inc} , and the outgoing particle energy, E_{out} , is given in the Appendix.

The results from the calculation of the projected recoil ranges are not sensitive to fine details of the angular distributions of the emitted particles. Different procedures, for instance the use of angular distributions from the systematics of Kalbach and Mann,⁹ are not expected to lead to significantly different results.

The angular distribution of particles evaporated from excited nuclei after a preequilibrium emission was assumed to be isotropic.

The linear momentum of a given final residue, after a series of emissions, is simply calculated by imposing linear momentum conservation at each emission. The projected momentum distribution is obtained in a Monte

Carlo approach by simulating the deexcitation cascade typically 20 000 times.

At the end of a cascade, the range of each fragment was calculated from a parametrization of the range/energy values reported by Northcliffe and Schilling¹⁰ for the range of that element in aluminum, applying mass scaling to obtain ranges for isotopes other than that listed.

In the construction of the final distribution, the recoils were assumed to originate with equal probability from all depths in the cobalt target. Allowance was made for the experimental effects of range straggling, beam energy spread, and catcher nonuniformity, by adding to the final projected range, r , a perturbation randomly selected from a Gaussian distribution with standard deviation equal to $a + br$. As suggested in Ref. 2, values of 0.08 mg cm⁻² and 0.025 were used for the constants a and b .

The other parameters used in the OMEGA calculation were exactly the same as reported in Ref. 3.

The previous conclusions, from analysis of excitation functions and angle integrated emitted particle spectra for reactions induced by α particles with energy up to ≈ 170 MeV on $A \approx 59$ nuclei, were that: (i) the code OMEGA provided a realistic and satisfactory description of the preequilibrium phase of the reaction, but (ii) the use of average parameters to describe the evaporation from the compound nucleus and the approximations introduced to speed up and simplify this part of the calculation prevented an accurate estimate of the cross section of processes with a predominant compound nucleus contribution, for nuclei as light as the ones considered in this work.

Because of (ii) we decided, in the present analysis, to evaluate the cross section of purely compound nucleus processes with the standard version of the code CASCADE,¹¹ using for the fusion cross sections the values for compound nucleus formation cross section estimated with the OMEGA code. These cross sections are estimated by evaluating the percentage of events in which the initial incident α particle energy is distributed among a large number of excitons (> 22), without previous emission of a preequilibrium particle.

For the four incident α particle energies considered in this work, the estimated compound nucleus formation cross sections are listed in Table II.

As shown in Fig. 5, an accurate reproduction of the experimental excitation functions is achieved. Comparison of the present results with those of Ref. 3 shows that the excitation functions of the reactions leading to the formation of ⁶¹Cu, ⁶⁰Cu, ⁵⁸Co, and ⁵⁷Co are now better reproduced, while the excitation function for production of ⁵⁶Co is slightly less accurately fitted.

TABLE II. Compound nucleus formation cross section for interaction of 38, 50, 65, and 85 MeV α particles with ⁵⁹Co.

E_α (MeV)	σ_{CN} (mb)
38	1011
50	912
65	755
85	524

The shapes of the recoil range distributions for purely compound nucleus processes were calculated by means of a Monte Carlo approach, described in Refs. 2 and 4, in which the emission of the prescribed number and type of particles with the appropriate Maxwellian distributions is simulated. Each evaporated nucleon is assumed to have an isotropic angular distribution in the c.m. system of the decaying nucleus; for evaporated α particles, equal contributions from isotropic and planar distributions with

$$\sigma(\theta, \phi) \approx \frac{1}{2\pi^2 \sin\theta} \quad (2)$$

were used.¹² In this case also the result of the calculation does not greatly depend on the assumed shape of the angular distributions. The use of second-order Legendre polynomials to reproduce the forward and backward peaking is expected to lead essentially to the same results.

As shown in Figs. 1–4, the measured recoil range distributions are well reproduced both in shape and absolute value, except in the case of ⁶⁰Cu and ⁵⁶Co at 85 MeV, where the calculation provides cross section values substantially greater than the values reported in Ref. 3. However, in considering these discrepancies, one should remember that there is significant uncertainty in the absolute value of the measured cross sections, which is reflected in the differences between values measured in different experiments.^{2,5}

Overall, the agreement between the calculated and measured distributions, in Figs. 1–4, must be considered remarkably good. These figures also show, in the case of reactions where an α particle may be emitted, the contribution of processes involving the emission of preequilibrium α particles. These results confirm that the exciton model calculations based on a realistic description of the α -nucleus interaction, which had previously correctly reproduced excitation functions and particle spectra, do indeed, with the same set of basic parameters, provide a quantitatively correct description also of the various reaction paths that contribute, at these energies, to each reaction.

IV. OTHER RECENT MEASUREMENTS OF MOMENTUM TRANSFER IN α -INDUCED REACTIONS

Jastrzebski *et al.*¹ have recently reported recoil studies of the same entrance channel at energies extending considerably higher (up to 200 MeV) than the measurements described in the previous two sections. For each radioactive product, they measured only the mean recoil range, as opposed to the full distribution, in a thick target/thick catcher experiment, and deduced the corresponding mean projected recoil momentum, \bar{p} , from range/energy relations.¹⁰ They also measured the total yield for each product mass (using in-beam γ spectrometry to establish yields of stable products).

Figure 7 shows the results obtained by these authors at 40, 66, 127, and 149 MeV for \bar{p}/p_{CN} and the total mass yield, as a function of ΔA , the difference between the mass of the compound nucleus (CN) and that of the product.

The estimates for these quantities calculated by the

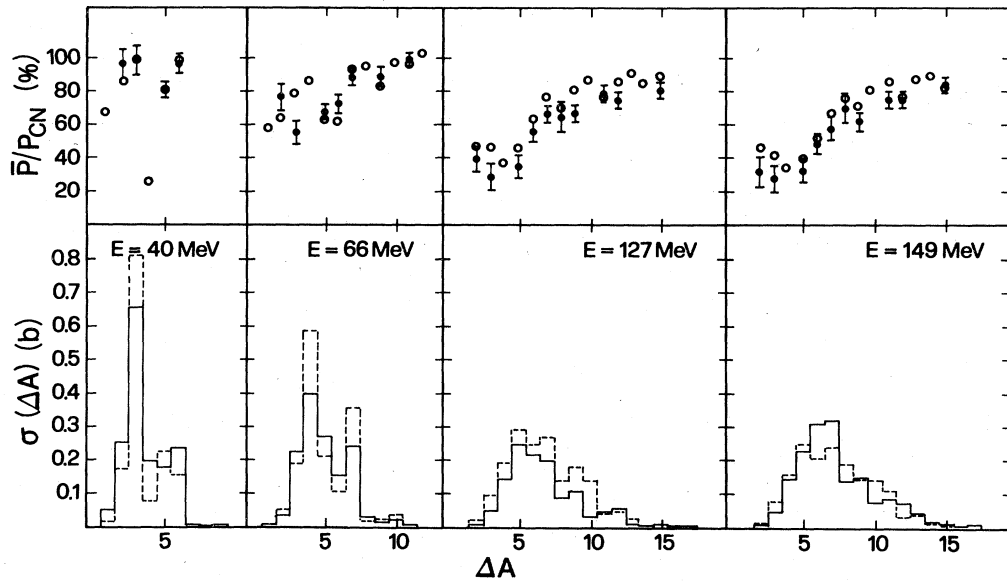


FIG. 7. Production cross sections of residue isobars and percentages of mean longitudinal linear momentum transferred to residue isobars in α -particle-induced reactions on ^{59}Co at 40, 66, 127, and 149 MeV. The experimental results (Ref. 1) are represented, respectively, by the continuous line histograms and black dots with error bars; the results of the present calculation are represented by dashed line histograms and open dots. \bar{p} represents the mean longitudinal linear momentum of the residue isobars, p_{CN} the initial α particle momentum, which would correspond to the mean longitudinal linear momentum transferred to each residue in a pure compound nucleus process. ΔA is the difference between the compound nucleus mass and the residue isobar mass.

OMEGA exciton model code are also shown in this figure. For these calculations, the code (modified as described in Sec. III) was used even for the purely compound nuclear processes, since the approximations discussed in Sec. III have little effect on the calculation of mass yields or recoil ranges, being important only in determining the relative yields of individual isobars.

As can be seen, the calculation satisfactorily reproduces the observed mass dependences, practically the sole exception being the value for $\Delta A=3$ at an incident α energy of 66 MeV.

In this particular case, it is quite surprising that the measured mean recoil momentum for $\Delta A=3$ is less than for $\Delta A=2$, since the contribution of preequilibrium processes is expected to be less in the first case than in the second. The drop in measured values for still lighter products is due to the importance of α emission in their production and demonstrates, as did the experimental recoil range distributions, the great influence of deep inelastic α particle scattering in reducing the mean linear momentum transferred to residual nuclei. At 66 MeV this drop does not occur for $\Delta A=4$, as at the other energies, because at this particular energy the yield is dominated by evaporation of just four nucleons which masks the preequilibrium emission of a single α particle.

It should also be noted that the values of \bar{p} obtained by Jastrzebski *et al.* are probably systematically high, by perhaps 5% in some cases, due to the method of obtaining the mean recoil velocity from a value of mean range for an extended distribution.

The dependence, on the incident α particle energy, of the longitudinal linear momentum transfer averaged over

all final products is also satisfactorily reproduced, as seen in Fig. 8.

As a result of this comparison, we find no evidence to support the conclusion of the authors of Ref. 1, that their data imply that the general character of the α -nucleus interaction changes quite abruptly at an energy corresponding approximately to 23 MeV/nucleon. We agree rather

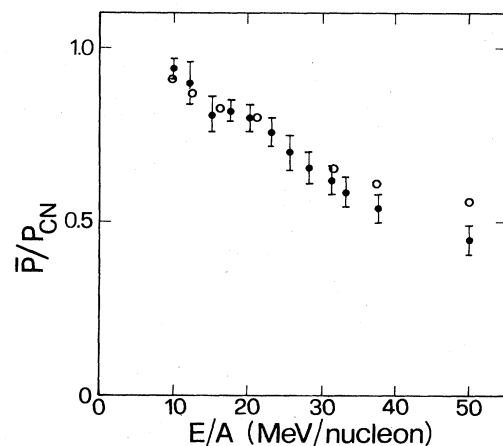


FIG. 8. Percentage of the mean linear momentum transfer in the reactions induced by α particles on ^{59}Co as a function of the incident energy/nucleon. Black dots with error bars represent the experimental values (Ref. 1), the open dots represent the results of the present calculation. \bar{p} is the longitudinal linear momentum averaged over all final residues, p_{CN} is the incident linear momentum.

with previous suggestions that there is no change in the general character of the light ion-nucleus interaction at energies up to ≈ 70 MeV/nucleon.¹³

V. CONCLUSIONS

Differential recoil range distributions have been measured for residual nuclei produced in reactions of alpha particles with ^{59}Co , at alpha energies between 38 and 85 MeV. These distributions show contributions that reflect the full momentum transfer in fusion/evaporation and the lower net momentum transfer resulting from various direct and preequilibrium processes.

The measured distributions are generally well reproduced, both in shape and in absolute cross section, by exciton model calculations, in which the possible initial interaction modes of the alpha particle with the target nucleus are all explicitly considered, using the same parameters as in previous calculations which successfully accounted for the product cross sections. This shows that these calculations correctly reproduce not only the cumulative cross sections, but also the balance of the various processes contributing to formation of each product.

These calculations also agree with the values of mean recoil range for these reaction residues measured by Jastrzebski *et al.* up to about 200 MeV in alpha energy.

Since this description accounts, uniformly across the energy range considered, for the experimental data, there are no grounds to support the suggestion of a change in the character of the alpha-nucleus interaction at incident energies below about 50 MeV/nucleon.

ACKNOWLEDGMENTS

Our thanks are due to Dr. P. E. Hodgson and Prof. J. J. Hogan for their continued interest and encouragement in this work and to Dr. J. Jastrzebski for exchange of information and enlightening discussions. This work has been partly supported by a grant of the Italian Ministry of Public Instruction.

APPENDIX

Analysis of the angular distributions of nucleons emitted in reactions induced by α particles up to about 140 MeV, on nuclei with $A \approx 60$, shows that one can assume an isotropic angular distribution for nucleons with energy smaller than 10 MeV. If their energy exceeds 10 MeV, one can assume an angular distribution of the type given by Eq. (1), with the function A given by:

$$\begin{aligned} A(E_{\text{inc}}, E_{\text{out}}) &= \frac{750}{E_{\text{out}}}, \quad E_{\text{inc}} \leq 55 \text{ MeV}, \\ &= \frac{750}{E_{\text{out}} - (0.0541E_{\text{inc}} - 2.9755)}, \quad E_{\text{inc}} > 55 \text{ MeV}. \end{aligned} \quad (\text{A1})$$

All the energies are given in MeV.

There is some indication that the angular distributions should somewhat flatten below $\approx 10^\circ$, and to simulate this occurrence, we have assumed

$$\sigma(\theta, \phi) \approx \sigma(\theta_{\text{min}}, \phi) \quad (\text{A2})$$

for $\theta < \theta_{\text{min}}$. However, a variation of θ_{min} from 0° to 10° has a small influence on the calculated recoil range distributions.

The analysis of angular distributions of emitted α particles prompted us to assume an isotropic angular distribution if the incident α energy is smaller than ≈ 32 MeV; for higher incident energies, an isotropic angular distribution was assumed for α particles emitted with less than 15 MeV, while, for higher emitted energies Eq. (1) was used, with the function A given by

$$\begin{aligned} A(E_{\text{inc}}, E_{\text{out}}) &= (1150. + 17.5E_{\text{inc}})e^{-(E_{\text{out}}/6)}, \quad 15 < E_{\text{out}} \leq 25 \text{ MeV}, \\ &= \frac{400. + 7.4E_{\text{inc}}}{E_{\text{out}}}, \quad E_{\text{out}} > 25 \text{ MeV}. \end{aligned} \quad (\text{A3})$$

Here again, for $\theta < \theta_{\text{min}}$ one has assumed the validity of (A2). In the case of alpha fragmentation, it has been assumed, for simplicity, that the heavy fragments (d, t, and ^3He) are emitted in the direction of the incident α particle, since in our approach the cross section for this pro-

cess gives a minor contribution to the total reaction cross section and the calculation is rather insensitive to the angular distribution of emitted particles for very forward emissions.

¹J. Jastrzebski, P. P. Singh, T. Mroz, H. J. Karwowski, S. E. Vigdor, and M. Fatyga, *Phys. Lett.* **136B**, 153 (1984).

²D. J. Parker, J. Asher, T. W. Conlon, and I. Naqib, *Phys. Rev. C* **30**, 143 (1984).

³E. Gadioli, E. Gadioli Erba, J. Asher, and D. J. Parker, *Z. Phys. A* **317**, 155 (1984).

⁴D. J. Parker, Ph.D. thesis, Oxford University Report AERE-R 11464, 1984.

- ⁵R. Michel and G. Brinkmann, Nucl. Phys. **A338**, 167 (1980).
⁶E. Gadioli and E. Gadioli Erba, Z. Phys. A **299**, 1 (1981).
⁷E. Gadioli, E. Gadioli Erba, J. J. Hogan, and B. V. Jacak, Phys. Rev. C **29**, 76 (1984).
⁸E. Gadioli, E. Gadioli Erba, and M. Luinetti, Z. Phys. A **321**, 107 (1985).
⁹C. Kalbach and F. Mann, Phys. Rev. C **23**, 112 (1981).
¹⁰L. C. Northcliffe and R. F. Schilling, Nucl. Data Tables **A7**, 233 (1970).
¹¹F. Pühlhofer, Nucl. Phys. **A280**, 267 (1977).
¹²T. Ericson, Adv. Phys. **9**, 425 (1960).
¹³F. Saint Laurent, M. Conjeaud, R. Dayras, S. Harar, H. Oeschler, and C. Volant, Phys. Lett. **110B**, 372 (1982).